CHAPTER 1

INTRODUCTION

1.INTRODUCTION

Tumour is an abnormal mass of tissue. Tumours can be benign or malignant (cancerous). There are hundreds of different types of tumours. Their names usually reflect the kind of tissue they arise in, and may also tell you something about their shape or how they grow. Diagnosis depends on the type and location of the tumour. Tumour marker tests and imaging may be used; some tumours can be seen (for example, tumours on the exterior of the z skin or felt (palpated with the hands).

A brain tumour occurs when abnormal cells from within the brain. There are two main types of tumours: malignant or non-cancerous tumours and benign tumours.

Cancerous tumour can be divided into primary tumours, which start within the brain and the secondary tumours, which have spread from elsewhere, known as brain metastasis tumours.

All the types of brain tumours may produce symptoms that vary depending on the part of the brain that is affected. These symptoms may include headaches, seizures, problems with vision, vomiting and mental changes. The headache is classically worse in the morning and goes away with vomiting. Other symptoms may include difficulty in walking, speaking or with sensations. As the disease progresses, unconsciousness may occur. Medical images plays a vital role in brain tumour. Early imaging methods invasive and sometimes dangerous, Pneumoencephalography and cerebral angiography have been abandoned in favour of non-invasive, high resolution techniques.

The brain is an important organ that controls thought, memory, emotion, touch, motor skills, vision, respiration, body temperature, hunger, and many other processes that regulate our body. The spinal cord is a large bundle of nerve fibers that extends from the base of the brain to the lower back. It carries messages to and from the brain and the rest of the body.

A brain tumour is a growth of abnormal cells inside the brain. Most brain tumours that children get are called primary brain tumours, meaning that they originated in the brain and did not spread from somewhere else. Tumours might be localized, remaining in one area, or they might be invasive, spreading into nearby tissues. Tumours are also categorized as benign (non-cancerous) or malignant (cancerous). However, it is difficult to call any brain tumour "benign", because all can cause serious problems.

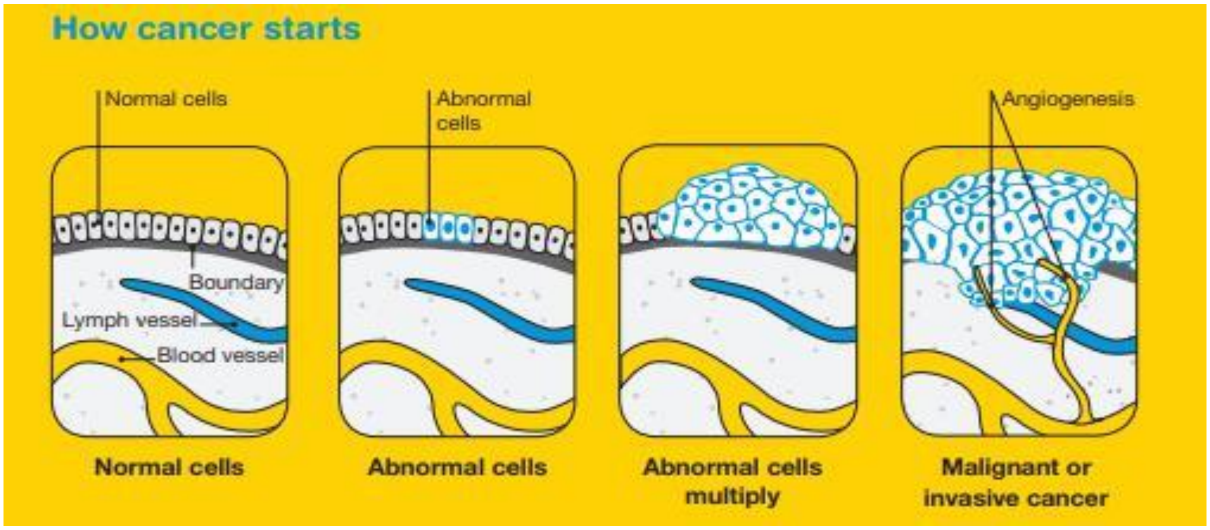

Fig 1.1 Tumour development stages

1.1 BRAIN CANCER STATISTICS:

A primary brain or spinal cord tumour is a tumour that starts in the brain or spinal cord. This year, an estimated 23,880 adults (13,720 men and 10,160 women) in the United States was diagnosed with primary cancerous tumours of the brain and spinal cord. Brain tumours account for 85% to 90% of all primary CNS tumours. Also, about 3,560 children will be diagnosed with a brain or CNS tumour this year.

Brain and other nervous system cancer are the 10th leading cause of death for women. It is estimated that 16,830 adults (9,490 men and 7,340 women) will die from primary cancerous brain and CNS tumours this year.

The 5-year survival rate tells you what percent of people lived at least 5 years after the tumour is found. Percent means how many out of 100. The 5-year survival rate for people with cancerous brain or CNS tumours is 34% for men and 36% for women. However, survival rates vary widely and depend on several factors, including the type of brain or spinal cord tumour. Talk with your doctor about what to expect with your diagnosis.

Brain cancer was the 18th most commonly diagnosed cancer in Australia in 2014. It is estimated that it will become the 17th most commonly diagnosed cancer in 2018.

In 2016, there were 1,439 deaths from brain cancer in Australia (878 males and 561 females). In 2018, it is estimated that there will be 1,435 deaths (856 males and 579 females). In 2018, it is estimated that the risk of an individual dying from brain cancer by their 85th birthday will be 1 in 157 (1 in 128 males and 1 in 200 females).

The number of new cases of brain cancer diagnosed increased from 853 (491 males and 362 females) in 1982 to 1,710 in 2014. Over the same period, the age–

standardised incidence rate increased from 6.3 cases per 100,000 persons (7.5 for males and 5.1 for females) in 1982 to 6.7 cases per 100,000 in 2014.

The number of deaths from brain cancer increased from 391 (246 males and 145 females) in 1968 to 1,439 in 2016. Over the same period, the age–standardised mortality rate increased from 3.6 deaths per 100,000 persons (4.6 for males and 2.7 for females) in 1968 to 5.3 deaths per 100,000 in 2016.

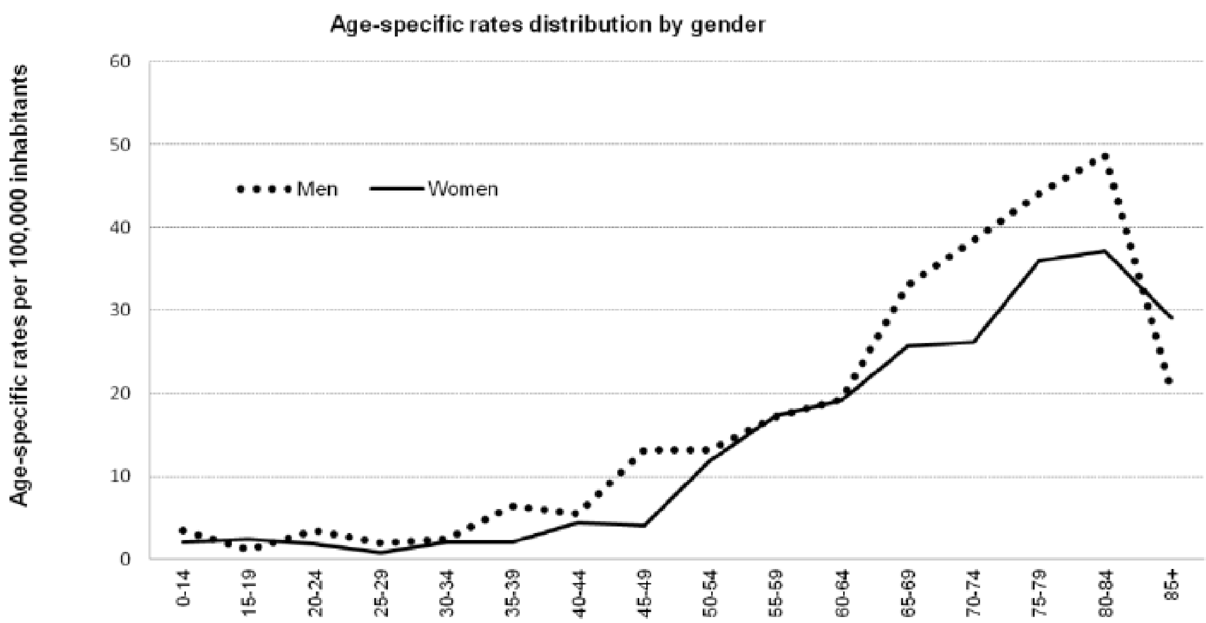

Figure 1.2 Brain Cancer Statistics

Source: American Society of Clinical Oncology (ASCO).
Link: https://www.cancer.net/cancer-types/brain-tumour/statistics

National Brain Tumour Society
Link: http://blog.braintumour.org/brain-tumour-facts-figures-may-2018-incidence-mortality-and-survival-in-2018/

1.2 TYPES OF BRAIN TUMOUR

Benign tumour: This kind of tumour is not cancer. It tends to grow slowly. Most benign brain tumours don't grow into nearby tissue. Once removed, they usually don't grow back. A benign tumour can cause symptoms like a malignant tumour depending on its size and location in the brain.

Malignant tumour: This kind of tumour is cancer. It usually grows fast, and grows into nearby tissue. This can make it hard to remove fully. A malignant brain tumour may grow back after treatment.

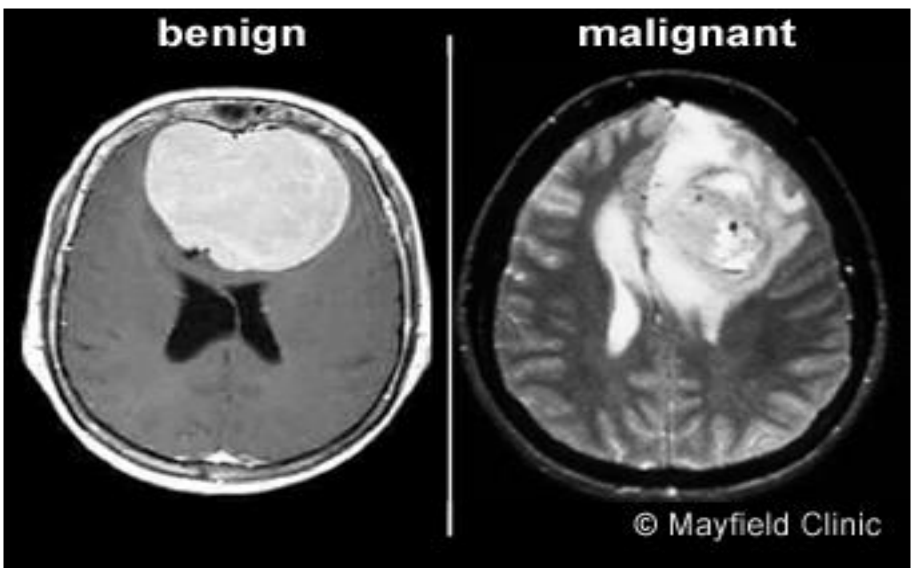

Figure 1.3 Brain Tumour Images

Brain tumours can be classified into two general groups:

- Primary brain tumour
- Secondary brain tumour

1.2.1 PRIMARY BRAIN TUMOUR

Primary brain tumours are named by the type of brain tissue where they're found. The most common type of primary brain tumour is a glioma. This type begins in the supportive (glial) tissue of the brain. Some gliomas tend to grow slowly. Others grow and spread quickly.

Some types of glioma include:

Astrocytoma: This kind of tumour comes from small star-shaped cells called astrocytes. In adults, an astrocytoma usually grows in the cerebrum. In children, they can grow in the cerebellum, cerebrum, and brain stem. Most astrocytoma's spread into nearby normal brain tissue and are hard to cure with surgery. Glioblastoma is a type of astrocytoma that tends to grow very quickly.

Brain stem glioma: This kind of tumour of the brain stem is more common in children than in adults. Because the brain stem controls many important functions, such as breathing and heart rate, this kind of tumour usually can't be removed by surgery.

Ependymoma: This kind of tumour starts in cells that line the fluid-filled spaces within the brain (ventricles). It doesn't often grow into nearby brain tissue. This means in some cases it can be cured with surgery.

Oligodendroglioma: This kind of tumour starts in cells that make myelin, the fatty substance that surrounds nerve cells. Like an astrocytoma, this tumour tends to spread into nearby brain tissue and is often hard to cure with surgery.

Optic nerve glioma: This kind of tumour grows in or around the nerve that sends messages from the eyes to the brain. This can cause vision changes. It can also cause hormone changes, due to its location near the pituitary gland. Other types of primary tumours include:

Primitive Neuroectodermal Tumour (PNET): This kind of tumour grows more often in children. It can grow anywhere in the brain in the primitive form of nerve cells. One type is the medulloblastoma. This kind of tumour is found in the cerebellum. They are more common in children than in adults. They tend to grow and spread quickly, but they can often be treated effectively.

Tumour of the pineal gland: This kind of tumour grows in and around the pineal gland. This is a tiny organ near the centre of the brain. The tumour can be slow-growing, called pineocytoma. Or it can be fast-growing, called pine blastoma.

Pituitary tumour: This kind of tumour starts in the pituitary gland at the base of the brain. It is almost always benign. But it can cause serious symptoms because of its location, and because it may secrete excess hormones.

Craniopharyngioma: This kind of tumour starts near the pituitary gland. It is usually slow growing. But it can cause symptoms if it presses on the pituitary gland or on nearby nerves.

Schwannoma: This kind of tumour starts in myelin-making cells that surround certain nerves. It's most common in the vestibular nerve in the inner ear that helps with balance. If it grows there, the tumour is called a vestibular schwannoma or an acoustic neuroma. This type of tumour is usually benign.

Meningioma: This kind of tumour starts in the outer linings of the brain (meninges). It is more common in adults. Many meningiomas can be removed with surgery, but some may grow back.

Primary central nervous system lymphoma: This is an aggressive, rare type of tumour that starts in lymphocytes. This is a type of immune cell. The tumour is more common in people with a disease of the immune system, such as AIDS. But it can grow in healthy people.

1.2.2 SECONDARY BRAIN TUMOUR

A secondary brain tumour is also known as a metastatic brain tumour. This is cancer that starts in another organ and then travels to the brain. In adults, secondary brain tumours are more common than primary brain tumours. Cancer in the brain that has spread from another part of the body is not considered brain cancer. It is still the same type of cancer as where it started. For example, lung cancer that has spread to the brain is called metastatic lung cancer.

These are some of the most common types of cancer that spread to the brain:

- Lung cancer
- Breast cancer
- Melanoma
- Colon cancer
- Kidney cancer

1.3 ORGANISATION OF THE PROJECT REPORT

Chapter 2: Deals with the previously proposed method and their disadvantages in the methods, and the need to choose a new method.

Chapter 3: Details about the microstrip patch antenna for biomedical applications. The simulation results about the patch antenna using Computer Simulation Technology (CST) Software have been discussed. Then about Hardware description also discussed.

Chapter 4: Deals with Experiments results and conclusion, we have done both the hardware and software experiments and the results have been successfully verified.

Chapter 5: Conclusion of our project have been explained here and future improvement of the project is also well explained.

CONCLUSION

Hence the proposed method for detecting brain tumour using Specific Absorption Rate of the microstrip antenna. Here the human brain cells Specific Absorption Rate will be taken as input so that we can identify the tumour cells. This work has introduced one brain tumour detection method to increase the accuracy and yield and decrease the diagnosis time and mainly decrease the side effects caused due to the radiation. The goal is to detect tumour cells from the Brain. The Specific Absorption Rate of human cells and tumour cells are different, this easily helps the identification of tumour. The frequency sent from the patch antenna is absorbed at a high rate by the tumour cells than healthy human cells. By this we can find the presence of tumour cells.

CHAPTER 2
LITERATURE REVIEW

2.1 INTRODUCTION

Literature review is an assignment of previous task done by various authors and collection of information or data from research papers published in journals to progress our task. There are lot of literatures published before on the same task. Some papers are taken into consideration from which idea of the project is taken.

2.2 WORK PROPOSED BY VARIOUS AUTHORS

- **Microwave System for Head Imaging**

A wideband microwave system for head imaging is presented. The system includes an array of 16 corrugated tapered slot antennas that are installed on an adjustable platform. A switching device is used to enable the antennas to sequentially send a wideband 1–4 GHz microwave signal and capture the backscattered signals. Those signals are recorded using suitably designed virtual instrument software architecture. To test the capability of the system to detect brain injuries, a low-cost mix- ture of materials that emulate the frequency-dispersive electrical properties of the major brain tissues across the frequency band 1–4 GHz are used to construct a realistic-shape head phantom. A target that emulates a realistic haemorrhage stroke is fabricated and inserted in two different locations inside the fabricated head phantom. A pre-processing algorithm that utilizes the symmetry of the two halves of human head is used to extract the target response from the background reflections. A post-processing confocal algorithm is used to get an image of the phantom and to accurately detect the presence and location of the stroke.

- **Dual-Polarized, Broadside, Thin Dielectric Resonator Antenna for Microwave Imaging**

We present a design for a dielectric resonator antenna (DRA) with dual-polarization characteristics. This antenna is de- signed for use in a three-dimensional (3-D) microwave to mography system to collect co-polar and cross-polar responses. The broadside radiation and dual polarization are achieved by exciting the fundamental mode of the DRA as well as by using two elements of the DRA that are perpendicular to each other. Compared to the conventional rectangular DRA, the proposed antenna is reduced in size by a factor of 6.7. The proposed DRA offers a measured bandwidth of 72% (2.6–5.52 GHz). The performance and radiation characteristics of the antenna are verified experimentally.

- **A Compact Double-Layer On-Body Matched Bowtie Antenna for Medical Diagnosis**

A compact double-layer Bowtie antenna optimized for medical diagnosis is presented in this paper. This on-body antenna is matched to the human body to allow more energy to be radiated into the human body to obtain stronger reflections for image processing. By using a Bowtie antenna with double layers as well as a folded structure and meandered micro strip lines at the bottom of the antenna, a small size of 30 30 mm with a size reduction of 40% is achieved, compared to the reference antenna of 50 50 mm within the same operational frequency range. After the optimization of the antenna parameters, the antenna is characterized from 0.5 to2 GHz, where the low frequencies enable a high penetration into human body and the large frequency range contributes to a high bandwidth and hence a fine range resolution. The simulated and measured results are shown with respect to the impedance matching, near-field pattern, gain and SAR distributions. With features such as a very small size, very low operational frequency, high front-to-back ratio, this design shows a high potential for use in medical diagnosis of stroke, breast cancer and water accumulation detection in the human body.

- **Bandwidth Enhancement of a Microstrip-Line-Fed Printed Wide-Slot Antenna with a Fractal-Shaped Slot**

Microstrip-line-fed printed wide-slot antenna with a fractal- shaped slot for bandwidth enhancement is proposed and experimentally studied. By etching the wides lot as fractal shapes, it is experimentally found that the operating bandwidth can be significantly enhanced, and the relation between the bandwidth and the iteration order (IO) and iteration factor (IF) of the fractal shapes is experimentally studied. Experimental results indicate that the impedance bandwidth, defined by 10 dB reflection coefficient, of the proposed fractal slot antenna can reach an operating bandwidth of 2.4 GHz at operating frequencies around 4 GHz, which is about 3.5 times that of a conventional microstrip-line-fed printed wide-slot antenna. It also achieved a 2-dB gain bandwidth of at least 1.59 GHz.

- **Wideband Unidirectional Antenna of Folded Structure in Microwave System for Early Detection of Congestive Heart Failure**

A three-dimensional antenna based on a combination of loop and dual mono pole structures with parasitic elements is presented. The antenna is specifically designed for a microwave system aimed at the early detection of congestive heart failure. The antenna is first designed as a planar structure and then folded over optimally defined folding lines to properly alter the path and phase of the surface currents for a unidirectional radiation and compact size as needed for the detection system. A prototype antenna of size (where, is the wavelength of the lowest resonant frequency) is developed to cover the band required in the targeted application. The measured results indicate 53% fractional bandwidth (580 – 1000 MHz), 6-8 dB front to back ratio, and 3-5 dBi gain. The antenna is then used to build a heart failure detection system, which also includes a compact microwave transceiver, a processing and image re-constructionalgorithmbasedonthesyntheticaperturefocusingtechnique, and a display unit. The system is used to successfully detect an early case of congestive heart failure in an artificial torso phantom that includes the main torso organs.

CHAPTER 3

PROPOSED METHODOLOGY

3.1 INTRODUCTION

The proposed antenna is realized on Copper with PCB substrate with length=50mm, breath= 50mm and thickness h=2mm. The antenna is simulated using CST software. Microstrip patch antennas are fed by a variety of methods. This antenna is designed by using co-axial line feed as it is easier to fabricate.

3.2 SIMULATION SOFTWARE – CST

CST Microwave Studio is a specialist tool for the 3D EM simulation of high frequency components. The unparalleled performance from CST makes it the first choice in leading R&D departments, since it enables the fast and accurate analysis of high frequency (HF) devices such as antennas, filters, couplers, planar and multi-layer structures and SI and MWS quickly gives insight into the EM behavior of your high frequency designs.

3.2.1 CST SOFTWARE DESCRIPTION:

The antenna is designed and simulated in CST (Computer simulation technology) design software. CST is a commercial finite element method solver for electromagnetic structures. The acronym originally stood for high frequency structural simulator. It is one of several commercial tools used for antenna design, and the design of complex RF electronic circuit elements including filters, transmission lines, and packaging. CST offers accurate, efficient computational solutions for electromagnetic design and analysis. Our 3D EM simulation software is user friendly and enables you to choose the most appropriate method for the design and optimization of devices operating in a wide range of frequencies. It is based on Finite Element Method (FEM).

FEM has its origin in the field of structural analysis. It is a more powerful and adaptable numerical technique for handling programs involving complex 24 geometries. In mathematics, FEM is a numerical technique for finding approximate solutions to boundary value problems. It uses variation methods (the Calculus of variations) to decrease an error function and produce a steady solution. As we know that joining many tiny straight lines can approximate a larger circle, FEM involves all the methods for connecting many simple element equations over many small subdomains, named finite elements, to approximate a more complex equation over a larger domain. FEM analysis of any problem involves basically four steps Passive microwave and RF component design is a major application of CST and supporting it is one of CST ’s core competencies. CST MWS offers a broad range of solver technologies, operating in both the time and frequency domain and capable of using surface meshes as well as Cartesian and tetrahedral volume meshes. An antenna array allows us to achieve high gain with multiple radiating elements and a phased array in addition offers the possibility to shape and steer the beam without changing the array geometry.

3.2.2 FEATURES OF CST

- Native graphical user interface based on Windows XP, Windows Vista, Windows 7 and Linux.
- Fast and memory efficient Finite Integration Technique.
- Extremely good performance due to Perfect Boundary Approximation (PBA) feature for solvers using a hexahedral grid. The transient and Eigen mode solvers also support the Thin Sheet Technique (TST).

- The structure can be viewed either as a 3D model or as a schematic. The latter allows for easy coupling of EM simulation with circuit simulation.

3.2.3 ADVANTAGES OF CST

- Advanced ACIS based parametric solid modeling front end with excellent structure visualization.
- Feature based hybrid modeler allows quick structural changes.
- Structure templates for simplified problem description.
- Efficient calculation for loss-free and lossy structures.
- MPI Cluster parallelization via domain decomposition.
- Combined simulation with MPI and GPU acceleration.

3.3 HARDWARE DESCRIPTION:

MATERIAL USED: 'COPPER'

Copper is an excellent electrical conductor. Most of its uses are based on this property or the fact that it is also a good thermal conductor. However, many of its applications also rely on one or more of its other properties. For example, it wouldn't make very good water and gas pipes if it were highly reactive. On this page, we look at these other properties:

- a good electrical conductor

- a good thermal conductor
- corrosion resistant
- antibacterial
- easily joined
- ductile
- tough
- non magnetic
- attractive colour
- easy to alloy
- recyclable
- catalytic

3.3.1 Corrosion resistant

- Copper is low in the reactivity series. This means that it doesn't tend to corrode. Again, this is important for its use for pipes, electrical cables, saucepans and radiators.

- However, it also means that it is well suited to decorative use. Jewellery, statues and parts of buildings can be made from copper, brass or bronze and remain attractive for thousands of years.

3.3.2 Antibacterial

- Copper is a naturally hygienic metal that slows down the growth of germs such as E-coli (the “burger bug”), MRSA (the hospital “superbug”) and legionella.

- This is important for applications such as food preparation, hospitals, coins, door knobs and plumbing systems.

3.3.3 Good Conductor

- Copper can be joined easily by soldering or brazing. This is useful for pipework and for making sealed copper vessel.

3.3.4 Substrate:

AIR is the substrate used in this microstrip antenna which acts as a very good transmission medium for the frequency which is radiated from the microstrip antenna.

3.4 BLOCK DIAGRAM

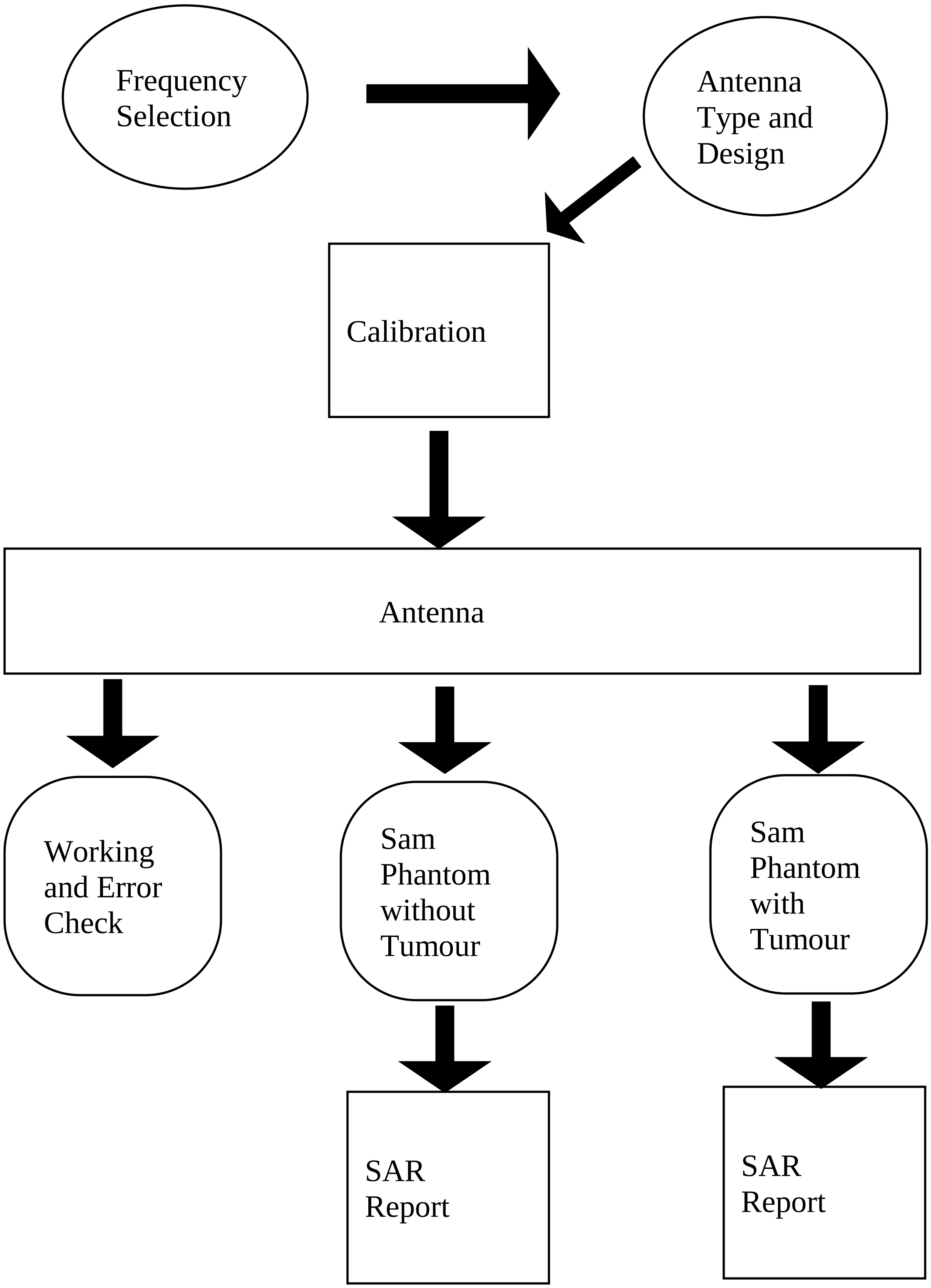

3.5. FREQUENCY SELECTION

As this is a low frequency antenna the operating frequency for this proposed microstrip antenna is from 2.4GHz to 2.7GHz which is in ISM band allocated for industry, study and research purpose by the Indian Government's rule. It is a low gain antenna which has gain around -10dB at 2.5GHz. The S-Parameter of the microstrip antenna show the correct frequency of the microstrip antenna which can be easily viewed in the CST software under the 1D result column.

3.6 ANTENNA TYPE AND DESIGN

We need to design a low frequency antenna which doesn't have any side effects and low power consumption we choose microstrip patch antenna because of its body wearing type and light weight. As it is said in Chapter 1 Microstrip antenna are easy to design and fabricate. The feeding method we used is the co-axial feed which is easy to feed a microstrip antenna and probably the best method to feed a low frequency microstrip patch antenna.

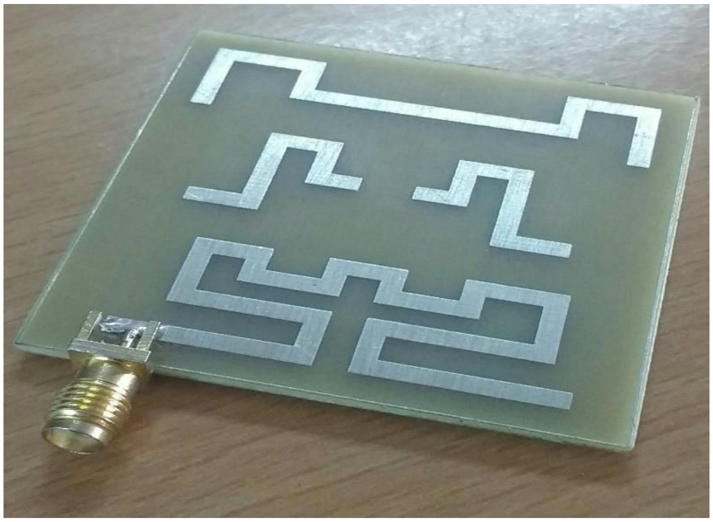

Fig.3.1 Microstrip Patch Antenna.

3.7. CALIBRATION

This method is mainly done in hardware to ensure that there is no error in the Network Analyzer to which the Microstrip antenna is connected through the feeding point. There are three different components in it they are,

- Load,
- Short,
- Open.

Fig3.2 Types of Calibration

3.7.1 LOAD

It is connected to feeding point of the network analyzer. The load is made of a small stainless-steel bullet like structure, which is 50 ohms in resistance. This is then virtually calibrated with a computer to which the network analyzer is connected.

3.7.2 SHORT

Same as Load, Short is another type of calibration connected to the feeding point of the network analyzer. It is also made up of stainless-steel. The resistivity of short is 0 (zero) ohms resistance because of its short circuit performance.

3.7.3 OPEN

Open is final calibration connected to the network analyzer. It has a resistance of infinite ohms resistance, because of its open circuit performance. It is also made up of stainless steel.

3.8 ANTENNA

The proposed antenna is made up of copper on a printed circuit board which has patches of 3 different kinds. The patches are named as EBG structured patch antenna. Which has 3 patches in the shape of 'E','B' and 'G'. Higher the length of the patch lower the operating frequency of the patch antenna. The 'E' shape has large length of 161mm. The 'B' shape has the length of 39mm. The 'G' shape patch is of length is 82mm.

3.9 WORKING AND ERROR CHECK

Before working with human head model, the antenna is checked for zero error and if the error is found the error is eliminated using bit error rate.

3.10 SAM PHANTOM WITHOUT TUMOUR

The human head without the tumour in it is used here for detection of the SAR value of the normal human cells or healthy human cells. Sam phantom is nothing but the human head model used in the CST software modelling method.

Here the antenna is placed at a distance of 60mm or 6 cm because the most effective radiance distance covered by it is at 60mm from the antenna. This helps the SAR calculation to have a maximum SAR point of 1.6W/kg or above which is widely required for the detection of Brain tumour in the human head.

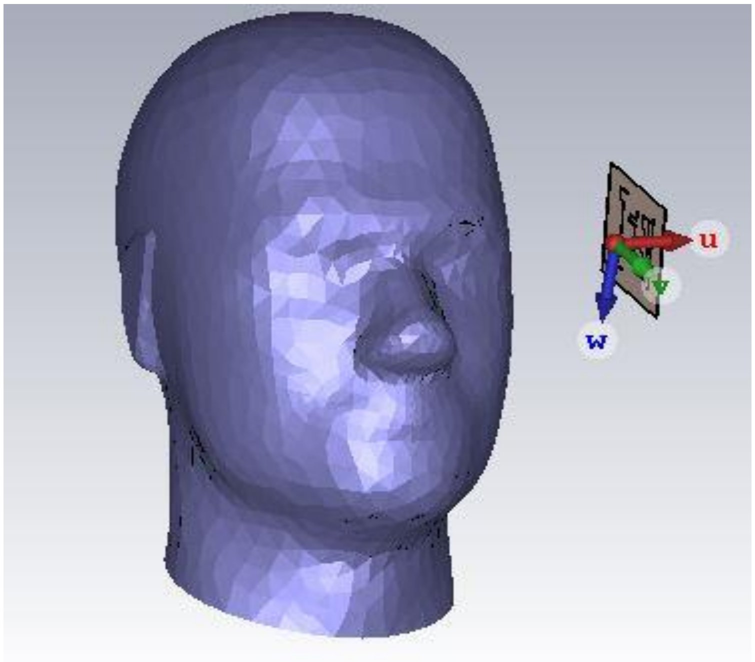

Fig.3.3 SAM PHANTOM WITHOUT TUMOR

3.10.1. SAR REPORT

After placing the antenna near the head of the healthy human we can start feeding the microstrip antenna. In CST software, we can start the stimulation process and finally the report is automatically generated by the CST software which can be viewed with the help of XPS viewer.

Min (x,y,z) [mm]:	-458.62, -474.741, -774.741
Max (x,y,z) [mm]:	833.36, 774.741, 474.741
Volume [mm^3]:	2.22313e+009
Absorbed power [W]:	9.91352e-008
Tissue volume [mm^3]:	5.24992e+006
Tissue mass [kg]:	5.24992
Tissue power [W]:	8.46537e-008
Average power [W/mm^3]:	1.61248e-014
Total SAR [W/kg]:	1.61248e-008
Max. point SAR [W/kg]:	1.67883e-005

Fig3.4 SAR REPORT WITHOUT TUMOUR

3.11 SAM PHANTOM WITH TUMOR

The Sam Phantom is nothing but the human head model which may or may not contains tumour cells depending on the user requirement. Same as the head inserted in it that file even tumour can be inserted in it. The Specific absorption rate of the frequency of signals sent by the microstrip patch antenna is at very different rate compared to the specific absorption rate a healthy human’s brain cells. This is mainly because of the tumor cells which behave at different character at different time thus it has a very much difference in the specific absorption rate.

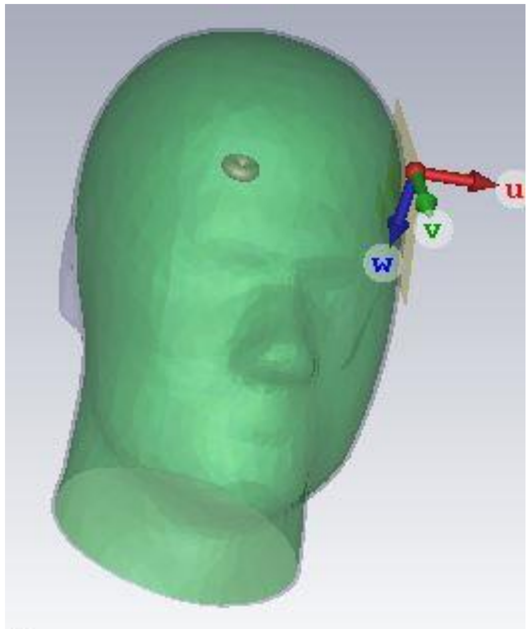

Fig 3.5 SAM PHANTOM WITH TUMOUR

3.11.1. SAR REPORT

Same as the report for Sam phantom without tumor is generated by the CST stimulation software itself is the SAR report of the for the Sam phantom with tumor. This report is generated as soon as we start the stimulation of the CST file where the microstrip antenna is placed at a distance of 60mm from the Sam phantom or the human head the antenna starts to radiate the signal which is absorbed by the Cancer cells at different ratio.

Min (x,y,z) [mm]:	-458.62, -474.741, -774.741
Max (x,y,z) [mm]:	833.36, 774.741, 474.741
Volume [mm^3]:	2.13909e+009
Absorbed power [W]:	3.01756e-005
Tissue volume [mm^3]:	5.24992e+006
Tissue mass [kg]:	5.25
Tissue power [W]:	2.87697e-005
Average power [W/mm^3]:	5.48003e-012
Total SAR [W/kg]:	5.47995e-006
Max. point SAR [W/kg]:	0.00610628

Fig.3.6 SAR REPORT WITH TUMOUR

CHAPTER 4

EXPERIMENTAL RESULTS AND DISCUSSION

4.1 INTRODUCTION

In this chapter, description of the results obtained through the proposed model. The working of the model is detailed in this chapter. CST is the software used to implement the proposed model.

4.2 EXPERIMENT

We need to design a low frequency antenna which doesn’t have any side effects and low power consumption we choose microstrip patch antenna because of its body wearing type and light weight. As it is said in Chapter 1 Microstrip antenna are easy to design and fabricate. The feeding method we used is the co-axial feed which is easy to feed a microstrip antenna and probably the best method to feed a low frequency microstrip patch antenna. We have done the experiment in CST Software, which is commonly used for Antenna design.

4.2.1 ANTENNA ERROR CHECK

Before Starting the stimulation of the antenna with the human head we should ensure that there is no error in it. Thus, it this method is used to eliminate the error in the antenna.

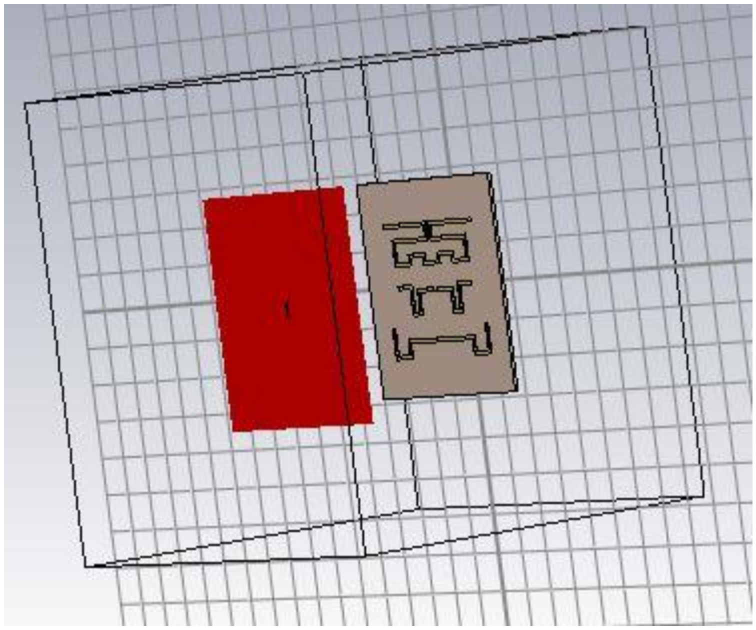

Fig 4.1 STIMULATED ANTENNA

The microstrip patch antenna is designed and stimulated as shown in the figure below and the S-parameters of the microstrip patch antenna is the output required to find the working status of the microstrip patch antenna.

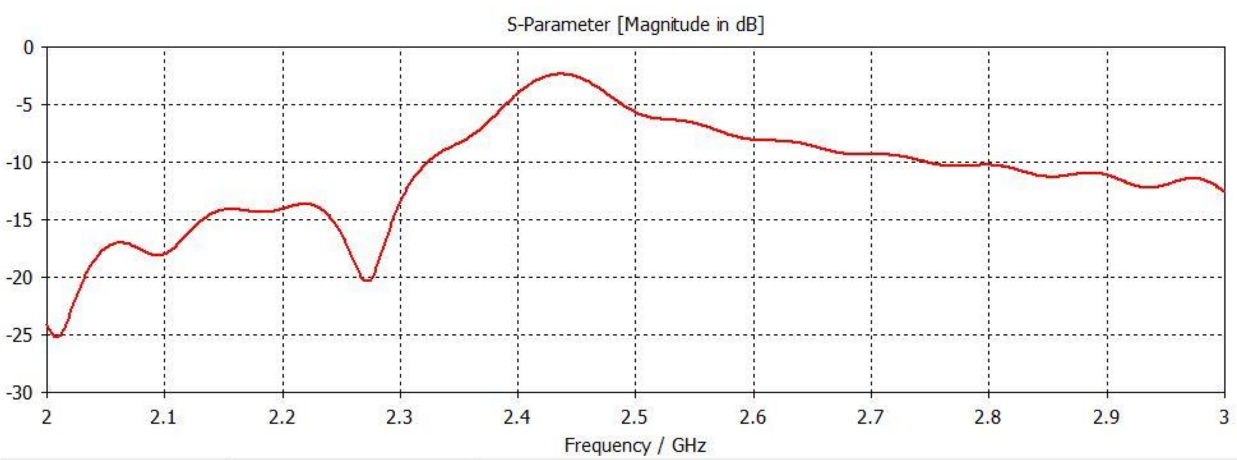

Fig4.2 S PARAMETER GRAPH

4.2.2. SAM PHANTOM WITHOUT TUMOUR

Now the working microstrip patch antenna is placed near the human head at a distance of 60mm, to achieve the maximum radiation intensity of the microstrip antenna. The image given below is the Sam phantom without tumor.

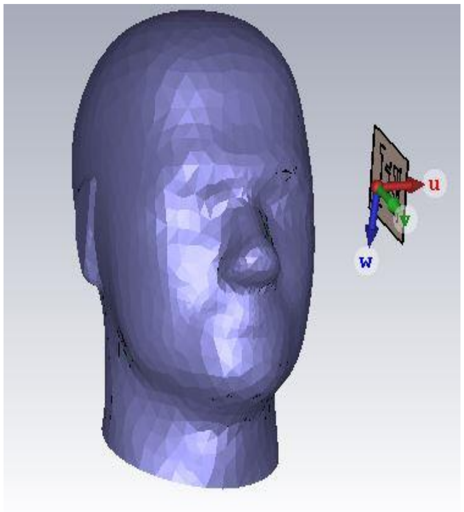

Fig. 4.3 SAM PHANTOM WITHOUT TUMOUR

The S-Parameter is given below is the graph that is generated by stimulating the file.

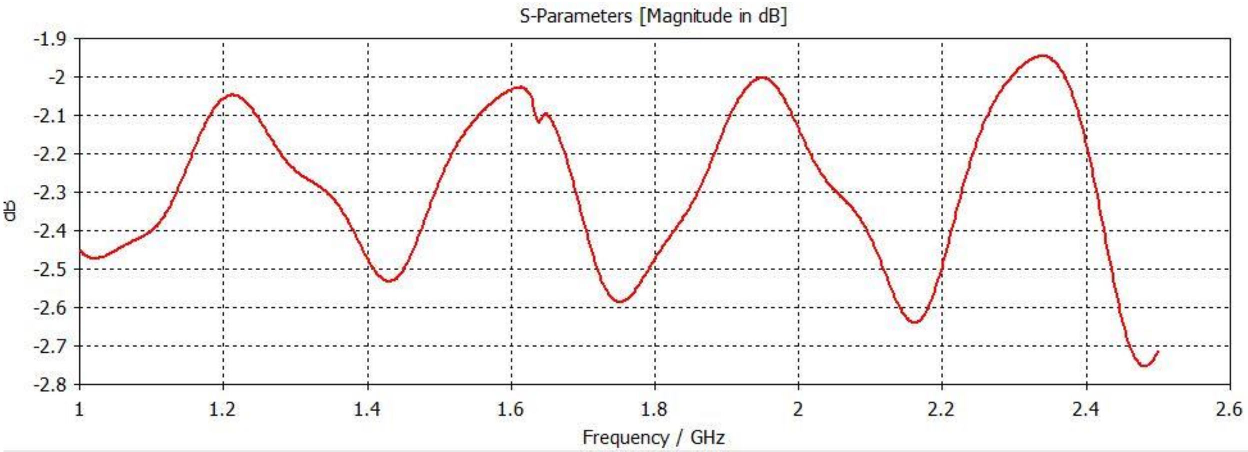

Fig4.4 SAM PHANTOM WITHOUT TUMOR S-PARAMETER GRAPH

Powerloss density monitor used: loss (f=3.25) [1] at 3.25 GHz

Power scaling [W] :	None
Stimulated Power [W] :	0.5
Accepted Power [W] :	0.495295
Average cell mass [g]:	0.239004
Averaging method:	IEEE/IEC 62704-1
Averaging mass [g]:	10

Entire Volume:

Min (x,y,z) [mm]:	-458.62, -474.741, -774.741
Max (x,y,z) [mm]:	833.36, 774.741, 474.741
Volume [mm^3]:	2.22313e+009
Absorbed power [W]:	9.91352e-008
Tissue volume [mm^3]:	5.24992e+006
Tissue mass [kg]:	5.24992
Tissue power [W]:	8.46537e-008
Average power [W/mm^3]:	1.61248e-014
Total SAR [W/kg]:	1.61248e-008
Max. point SAR [W/kg]:	1.67883e-005

Maximum SAR (10g) [W/kg]:	2.3938e-007
Maximum at (x,y,z) [mm]:	41.9061, 95.1025, 3.88218
Avg.vol.min (x,y,z) [mm]:	28.7336, 81.93, -15.9941
Avg.vol.max (x,y,z) [mm]:	55.0786, 108.275, 10.3509
Largest valid cube [mm]:	24.6852
Smallest valid cube [mm]:	21.5443
Avg.Vol.Accuracy [%]:	0.01

Calculation time [s]: 2

The above shown values are generated as a report by the CST file when stimulated. Maximum point Specific Absorption Rate is the required value for the identification of presence of tumour is the brain.

4.2.3 SAM PHANTOM WITH TUMOUR

The working microstrip patch antenna is placed near the human head at a distance of 60mm, to achieve the maximum radiation intensity of the microstrip antenna. The image given below is the Sam phantom with tumour.

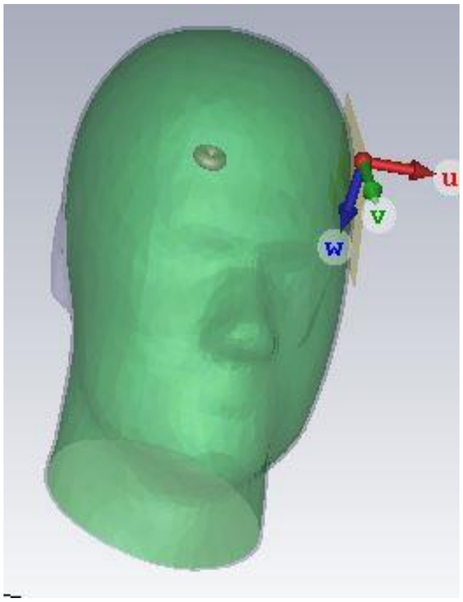

Fig. 4.5 SAM PHANTOM WITH TUMOUR

The S-Parameter is given below is the graph that is generated by stimulating the file.

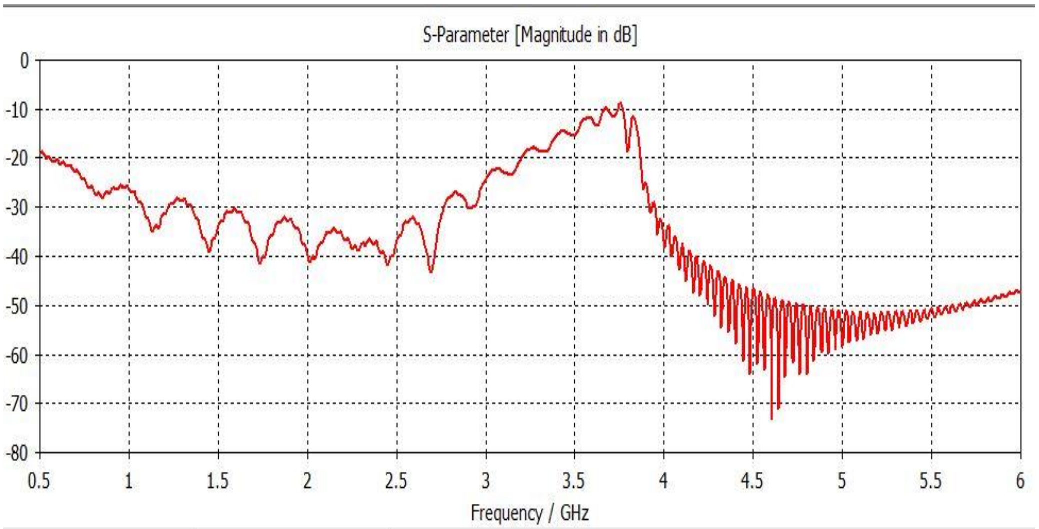

Fig4.6 SAM PHANTOM WITH TUMOUR S-PARAMETER GRAPH

```
Powerloss density monitor used: loss (f=2.7) [1] at 2.7 GHz
Power scaling [W] :           None
Stimulated Power [W] :        0.5
Accepted Power [W] :          0.499974
Average cell mass [g]:        0.0543158
Averaging method:             IEEE/IEC 62704-1
Averaging mass [g]:           10

--------------------------------------------------------------------------
----
Entire Volume:

Min (x,y,z) [mm]:             -458.62, -474.741, -774.741
Max (x,y,z) [mm]:             833.36, 774.741, 474.741
Volume [mm^3]:                2.13909e+009
Absorbed power [W]:           3.01756e-005
Tissue volume [mm^3]:         5.24992e+006
Tissue mass [kg]:             5.25
Tissue power [W]:             2.87697e-005
Average power [W/mm^3]:       5.48003e-012
Total SAR [W/kg]:             5.47995e-006
Max. point SAR [W/kg]:        0.00610628

Maximum SAR (10g) [W/kg]:     5.57132e-005
Maximum at (x,y,z) [mm]:      72.3735, 109.285, -155.927
Avg.vol.min (x,y,z) [mm]:     58.8969, 95.8084, -157.738
Avg.vol.max (x,y,z) [mm]:     85.8501, 122.762, -130.785
Largest valid cube  [mm]:     23.6305
Smallest valid cube [mm]:     21.4984
Avg.Vol.Accuracy    [%]:      0.01

--------------------------------------------------------------------------
----
Calculation time [s]:   12
```

The above shown values are generated as a report by the CST file when stimulated. Maximum point Specific Absorption Rate is the required value for the identification of presence of tumour is the brain.

4.3 FABRICATED ANTENNA

4.3.1 FRONT VIEW OF ANTENNA

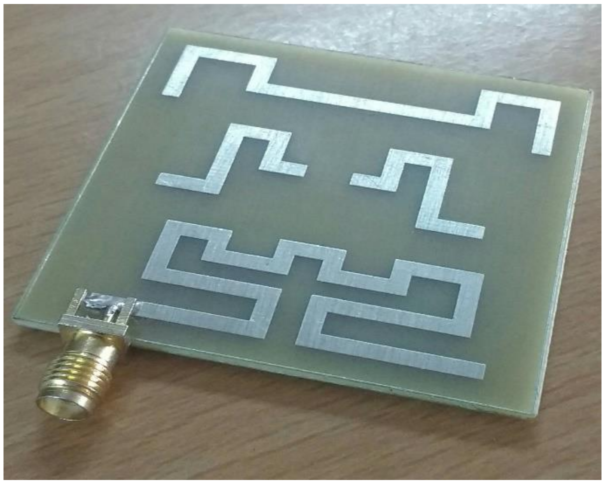

Fig. 4.7 FRONT VIEW OF ANTENNA

The above picture shows the front view of the fabricated antenna.

4.3.2 BACK VIEW OF ANTENNA

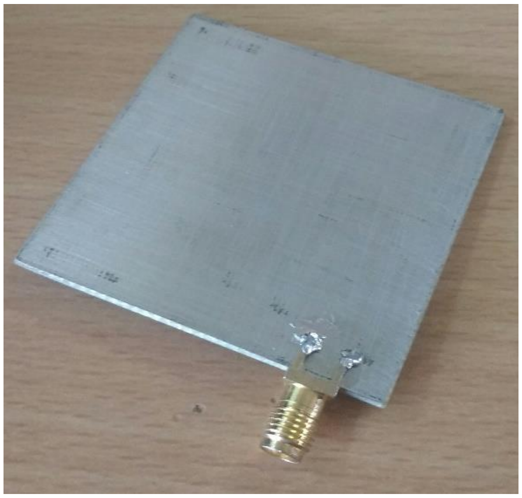

Fig. 4.8 BACK VIEW OF ANTENNA

The above shown image is the back view of fabricated antenna

4.4 RETURN LOSS

As we connect the network analyser with our microstrip antenna we get the return loss of our antenna. The below shown image is the return loss of the microstrip patch antenna we have designed.

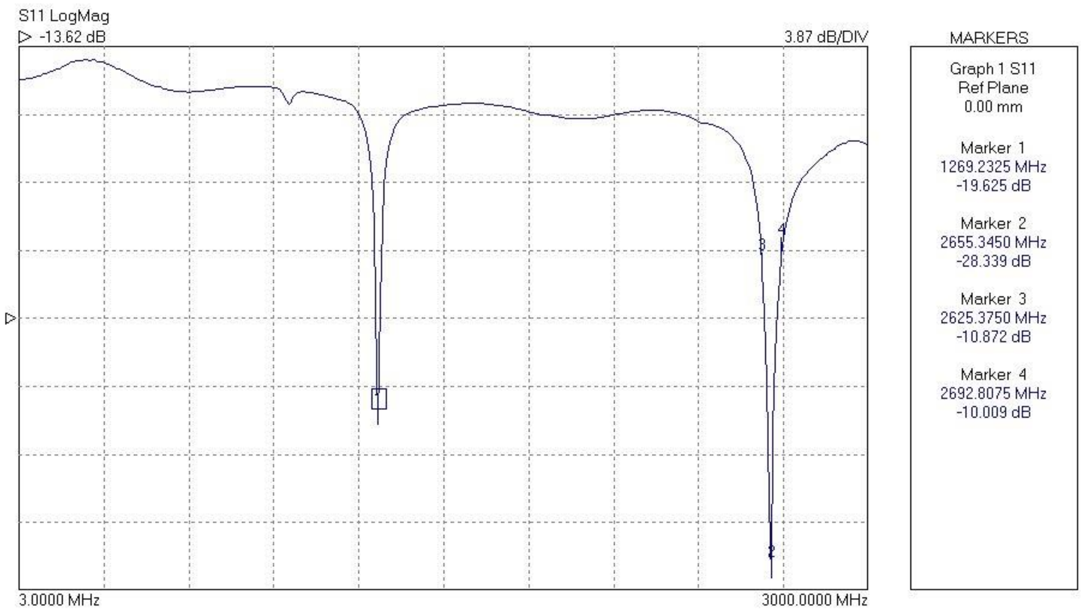

Fig. 4.9 RETURN LOSS GRAPH

Frequency (MHz)	Magnitude	Phase Shift
242.76	1.10879	-123.70
250.2525	1.07951	-127.94
257.745	1.0796	-132.28
265.2375	1.10211	-136.72

Tab. 4.1 RETURN LOSS TABLE

4.5 PHASE

By the same method we use to generate the return loss of the antenna we can also generate the phase of the microstrip patch antenna. The below shown image is the phase of the microstrip patch antenna we have designed.

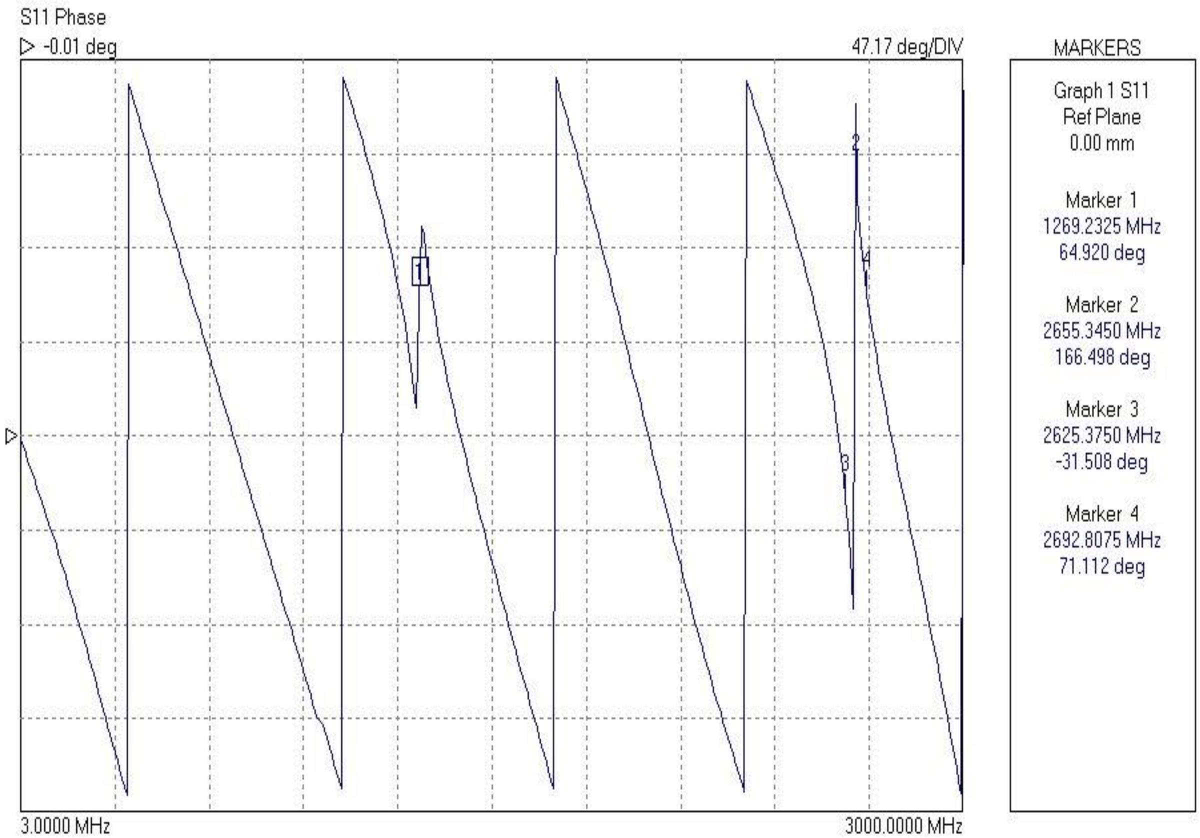

Fig.4.10 PHASE SHIFT GRAPH

4.6 SMITH CHART

By connecting the microstrip antenna with the network analyser, we can easily find the Smith Chart for our Antenna and its properties. The below shown image is the image of the smith chart for our microstrip patch antenna.

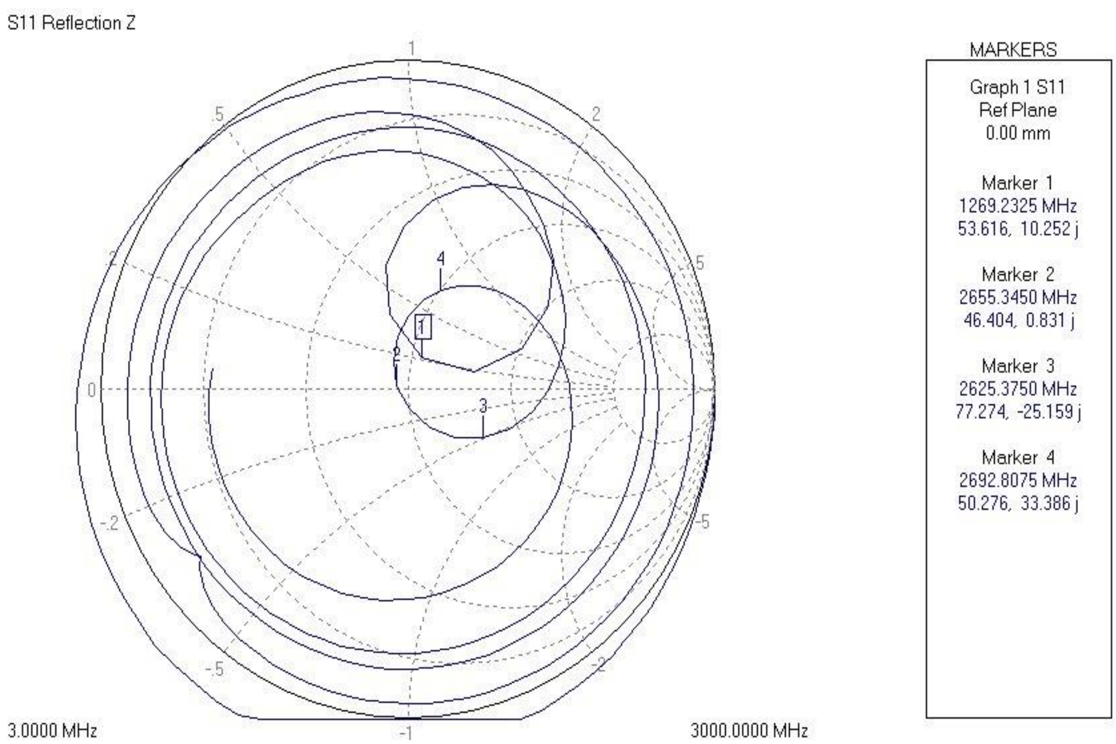

Fig. 4.11 SMITH CHART GRAPH

4.7 SWR

As soon as we finish connecting our microstrip patch antenna with the network analyser we can start the antenna operation and perform the SWR calculations of it.

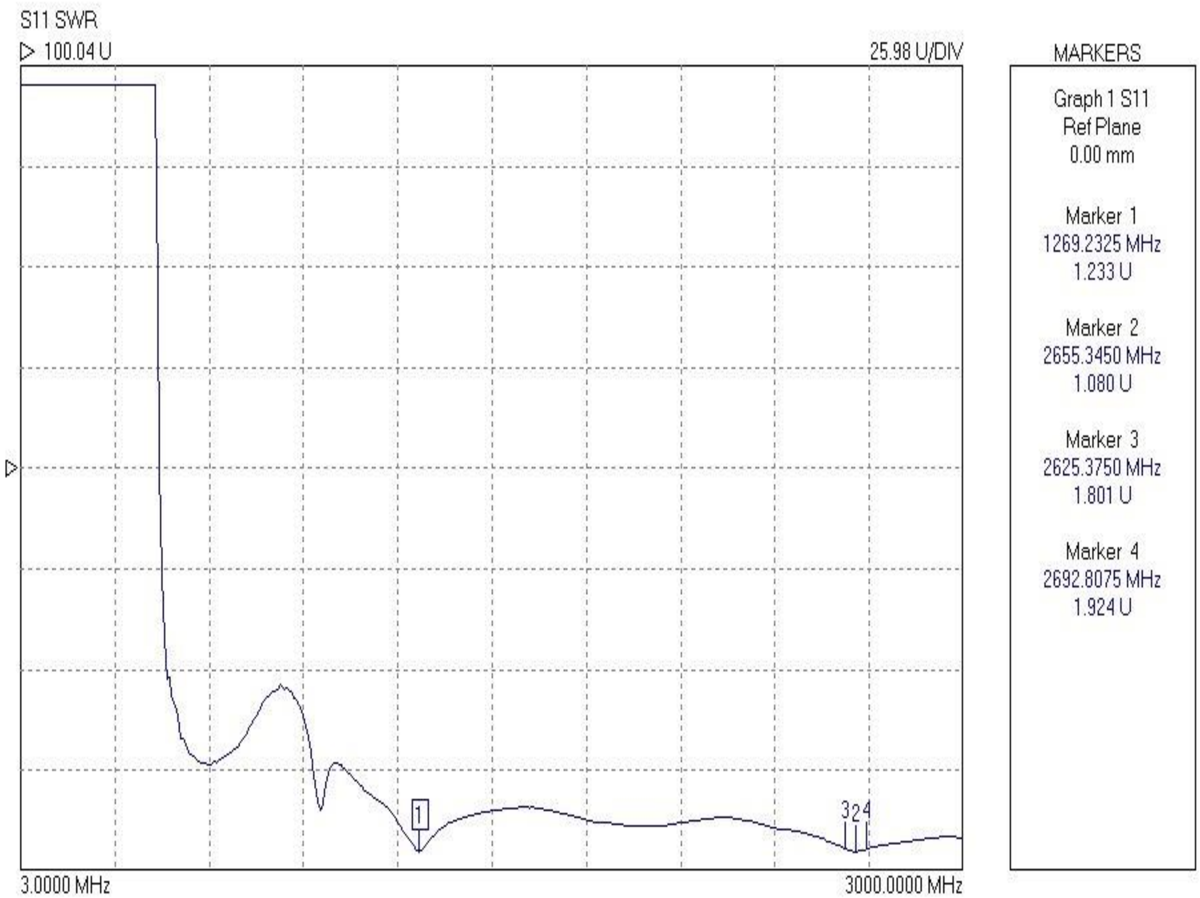

Fig.4.12 SWR GRAPH

CHAPTER 5

RESULT AND CONCLUSION

5.1 CONCLUSION

Thus, the proposed model includes the design and simulation of Microstrip patch antenna with little modifications in patch and ground in order to improve the bandwidth and directivity and it is fabricated on Teflon substrate with the help of copper. The human head phantom is designed with and without tumour, tested with the proposed antenna. The various response (with and without tumour) observed by the antenna and analyzed using CST software. From the response of simulated Specific absorption rate, we analyzed the statistical differences between the normal head and the head that contains tumor. From these results we were able to accurately find the presence of tumour.

5.2 FUTURE WORK

The future work of this project is to find the accurate position and size of tumour. By using different material as substrate, the gain, return loss, directivity can be further increased in order to analyze very minute sized tumours. A single microstrip antenna can be converted into an array of antenna which helps to attain the accurate size of the tumour. The output can also be made of visualizing in real time with the help of proper image processing and image segmentation.

REFERENCES

[1] B. J. Mohammed, A. M. Abbosh, S. Mustafa, and D. Ireland, "Microwave system for head imaging," *Instrumentation and Measurement, IEEE Transactions on,* vol. 63, pp. 117-123, 2014.

[2] o. N.-I. R. H. IEEE Standards Coordinating Committee 28, *IEEE Standard for Safety Levels with Respect to Human Exposure to Radio Frequency Electromagnetic Fields, 3kHz to 300 GHz*: Institute of Electrical and Electonics Engineers, Incorporated, 1992.

[3] A. Sabouni and A. Kishk, "Dual-polarized, broadside, thin dielectric resonator antenna for microwave imaging," *Antennas and Wireless Propagation Letters, IEEE,* vol. 12, pp. 380-383, 2013.

[4] A. T. Mobashsher, A. M. Abbosh, and Y. Wang, "Microwave system to detect traumatic brain injuries using compact unidirectional antenna and wideband transceiver with verification on realistic head phantom," *Microwave Theory and Techniques, IEEE Transactions on,* vol. 62, pp. 1826-1836, 2014.

[5] X. Li, M. Jalilvand, Y. L. Sit, and T. Zwick, "A compact double-layer onbody matched bowtie antenna for medical diagnosis," *Antennas and Propagation, IEEE Transactions on,* vol. 62, pp. 1808-1816, 2014.

[6] A. T. Mobashsher and A. Abbosh, "Slot-loaded folded dipole antenna with wideband and unidirectional performance for L-band applications," *Antennas and Wireless Propagation Letters, IEEE,* vol. 13, pp. 798-801, 2014.

[7] S. Ahdi Rezaeieh and A. Zamani, "3-D Wideband Antenna for HeadImaging System with Performance Verification in Brain Tumor Detection," *Antennas and Wireless Propagation Letters, IEEE,* vol. 14, pp. 910-914, 2015.

[8] C. Chiu, H. Wong, and C. Chan, "Study of small wideband folded-patchfeed antennas," *IET Microwaves, Antennas & Propagation,* vol. 1, pp. 501-505, 2007.

[9] T. Taga and K. Tsunekawa, "Performance Analysis of a Built-In Planar Inverted F Antenna for 800 MHz Band Portable Radio Units," *IEEE Journal on Selected Areas in Communications,* vol. 5, pp. 921-929, 1987.

[10] W.-L. Chen, G.-M. Wang, and C.-X. Zhang, "Bandwidth enhancement of a microstrip-line-fed printed wide-slot antenna with a fractal-shaped slot," *Antennas and Propagation, IEEE Transactions on,* vol. 57, pp. 2176-2179, 2009.

[11] S. Ahdi Rezaeieh, A. Abbosh, and Y. Wang, "Wideband unidirectional antenna of folded structure in microwave system for early detection of congestive heart failure," *Antennas and Propagation, IEEE Transactions on,* vol. 62, pp. 5375-5381, 2014.

[12] C. M. Kruesi, R. J. Vyas, and M. M. Tentzeris, "Design and development of a novel 3-D cubic antenna for wireless sensor networks (WSNs) and RFID applications," *Antennas and Propagation, IEEE Transactions on,* vol. 57, pp. 3293-3299, 2009.

[13] S. Ahdi Rezaeieh, A. Zamani, and A. Abbosh, "3-D Wideband Antenna for Head-Imaging System with Performance Verification in Brain Tumor Detection," *IEEE Antennas and Wireless Propagation Letters,* vol. 14, pp. 910-914, 2015.

[14] K. Foster, J. Schepps, R. Stoy, and H. P. Schwan, "Dielectric properties of brain tissue between 0.01 and 10 GHz," *Physics in medicine and biology,* vol. 24, p. 1177, 1979.

[15] S. Gabriel, R. Lau, and C. Gabriel, "The dielectric properties of biological tissues: II. Measurements in the frequency range 10 Hz to 20 GHz," *Physics in medicine and biology,* vol. 41, p. 2251, 1996.

[16] A. Peyman, S. Holden, S. Watts, R. Perrott, and C. Gabriel, "Dielectric properties of porcine cerebrospinal tissues at microwave frequencies: in vivo, in vitro and systematic variation with age," *Physics in medicine and biology,* vol. 52, p. 2229, 2007.

[17] M. Jalilvand, X. Li, L. Zwirello, and T. Zwick, "Ultra wideband compact near-field imaging system for breast cancer detection," *IET Microwaves, Antennas & Propagation,* 2015.

[18] R. K. Amineh, M. Ravan, A. Trehan, and N. K. Nikolova, "Near-field microwave imaging based on aperture raster scanning with TEM horn antennas," *Antennas and Propagation, IEEE Transactions on,* vol. 59, pp. 928-940, 2011.

[19] B. Menze et al., “The multimodal brain tumour image segmentation benchmark (brats),” IEEE Transactions on Medical Imaging, vol. 34, no. 10, pp. 1993–2024, 2015.

[20] Pereira, S., Pinto, A., Alves, V., et al.: ‘Brain tumour segmentation using convolutional neural networks in MRI images’, IEEE Trans. Med. Imaging, vol, 35, pp. 1240–1251,2016.

9TH INTERNATIONAL CONFERENCE ON SCIENCE AND INNOVATIVE ENGINEERING 2019

ORGANIZED BY

ORGANIZATION OF SCIENCE & INNOVATIVE ENGINEERING AND TECHNOLOGY, CHENNAI

IN ASSOCIATION WITH

JAWAHAR ENGINEERING COLLEGE, CHENNAI

Certificate of Presentation

This is to certify that Dr./Mr./Ms. BUVANESH. G from RAJALAKSHMI INSTITUTE OF TECHNOLOGY has presented a paper titled SMART ANTENNA FOR BRAIN TUMOUR APPLICATION in the "9th International Conference on Science and Innovative Engineering" held on 24th March 2019.

Secretary

Director

9TH INTERNATIONAL CONFERENCE ON SCIENCE AND INNOVATIVE ENGINEERING 2019

ORGANIZED BY

ORGANIZATION OF SCIENCE & INNOVATIVE ENGINEERING AND TECHNOLOGY, CHENNAI

IN ASSOCIATION WITH

JAWAHAR ENGINEERING COLLEGE, CHENNAI

Certificate of Presentation

This is to certify that Dr./Mr./Ms. BALAJI.V from RAJALAKSHMI INSTITUTE OF TECHNOLOGY has presented a paper titled SMART ANTENNA FOR BRAIN TUMOUR APPLICATION in the "9th International Conference on Science and Innovative Engineering" held on 24th March 2019.

Secretary

Director

9TH INTERNATIONAL CONFERENCE ON SCIENCE AND INNOVATIVE ENGINEERING 2019

ORGANIZED BY

ORGANIZATION OF SCIENCE & INNOVATIVE ENGINEERING AND TECHNOLOGY, CHENNAI

IN ASSOCIATION WITH

JAWAHAR ENGINEERING COLLEGE, CHENNAI

Certificate of Presentation

This is to certify that Dr./Mr./Ms. BALAJI. R from RAJALAKSHMI INSTITUTE OF TECHNOLOGY has presented a paper titled SMART ANTENNA FOR BRAIN TUMOUR APPLICATION in the "9th International Conference on Science and Innovative Engineering" held on 24th March 2019.

Secretary

Director